ELECTROLUMINESCENCE EXCITATION MECHANISMS IN AN EPOXY RESIN UNDER DIVERGENT AND UNIFORM FIELD

V. Griseri, L.A. Dissado, and J.C. Fothergill
University of Leicester, Department of Engineering, England

G. Teyssedre and C. Laurent
Université Paul Sabatier, Laboratoire de Génie Electrique, France

ABSTRACT

Electroluminescence excitation mechanisms have been investigated in epoxy resin under divergent and uniform field situations. Metallic wires embedded in the resin were used to produce field divergence whereas film samples were metallised to obtain a uniform field. Electroluminescence under divergent field was stimulated by an impulse voltage. Light was emitted on the positive and negative fronts of the square pulses when the field exceeded 20 kV/mm at the wire surface, with equal intensity and without polarity dependence. There was evidence of space charge accumulation around the wires in multiple-pulse experiments. Charge injection and extraction occurring at both fronts of the pulse provide the condition for EL excitation. Further excitation of the EL during the plateau of the voltage pulse is prevented by the opposite field of the trapped charge. Field computation with and without space charge supports the proposed interpretation. A DC voltage was used for the uniform field experiments. A continuous level of electroluminescence is found at 175 kV/mm. Charging/discharging current measurements and space charge profile analyses using the pulsed electro-acoustic (PEA) technique were performed at different fields up to the EL level. Dipolar orientation generates a long lasting transient current that prevents the conduction level being reached within the experimental protocol (one hour poling time). The continuous EL emission is nevertheless associated with a regime where the conduction becomes dominant over the orientational polarization. Polarization and space charge contribute to the PEA charge profiles. Homo-charge injection at anode and cathode is seen at 20 kV/mm and a penetration of positive space charge in the bulk is detected above 100 kV/mm, suggesting an excitation of the continuous EL by bipolar charge recombination.

1 INTRODUCTION

Electroluminescence (EL) will be defined in our context as the light emitted from a solid material when subjected to an electric stress. It results from the radiative relaxation of excited states that are created by the application of the field. These states can be delocalized when dealing with EL of semi-conducting materials [1,2], or highly localized when dealing with large band gap materials such as polymers used as insulation in electrical engineering [3]. In the latter case, it has been known for a long time that the existence of internal gas-filled cavities can also be at the origin of a light emission due to the excitation of gaseous molecules accompanying discharge occurrence [4]. In this paper, we will focus on the investigation of the light emitted by the material by taking care not to introduce any internal cavities of a size suitable to sustain partial discharges. This needs careful control during sample preparation.

EL detection in a given material is evidence of the generation of excited states of energy between ≈1.8 and ≈4.1 eV corresponding respectively to wavelengths of ≈700 nm and ≈300 nm. Because the excitation is localized on a particular site in the case of large band gap materials, excited states can be very reactive and promote chemical changes [5]. This is why EL is thought to be related to electrical ageing and dielectric breakdown of the material [3]. Moreover, its excitation needs to be facilitated by charge carriers, as the field by itself cannot promote electronic excitations in a good insulator. EL is therefore inherently linked to space charge [6] and can be used to gather information on processes such as charge injection, charge transport and charge dissipation.

The objective of this paper is to report on EL in epoxy resins, which are widely used as insulation in high voltage apparatus. A literature survey shows that there are very few reports on electroluminescence in epoxy. Most of the reported work concerns divergent field situations where needle electrodes have been molded into the resin [7-13]. Light emission was reported mainly under AC voltage application and was related to the early stage of electrical breakdown (electrical treeing initiation). In this study, we will focus on impulse and DC electroluminescence in divergent and uniform fields respectively.

The EL is associated with the generation of charge carriers within the polymer. These charges can be provided by injection, by de-trapping or by field-dissociation. The simplest mechanism of EL that can be envisaged follows the injection of charge carriers at an electrode contact. In the case of a unipolar injection of hot carriers, an impact ionization or excitation can lead to light emission by recombination of a pair of opposite charges or radiative relaxation of the neutral excited state, respectively. If a bipolar injection is taking place, either from the same contact under AC or from anode and cathode

under DC, then a process of recombination is expected in regions where positive and negative carriers can interact.

All these processes will depend on the type of space charge, its dynamics and spatial distribution. Studies aimed at detecting space charge in epoxy with some spatial resolution have recently been published. The build-up of space charge around wires molded into a resin measured using the Laser Induced Pressure Pulse (LIPP) method [14-16] has been reported. Short duration (5 to 150 ms), high voltage (up to 30 kV) pulses were applied to a set of gold-plated tungsten wires of 25 μm in diameter molded into the resin. It has been shown that charges can be transferred from the wires to the polymer whatever the polarity of the applied voltage. The amount of injected charge (nC range for wire length of the order of 1 cm) and the charge penetration depth (up to 80 μm away from the wire surface) depend on the parameters of the high voltage pulse but were observed to increase quickly for pulse duration between 5 to 20 ms. There is a near saturation in the amount of injected charge and penetration depth for longer pulse duration suggesting a space charge limited injection. On the other hand, the space charge distribution in films of epoxy subjected to a DC stress has been reported by using the Pulsed Electro-acoustic (PEA) method. From space charge profiles detected at different temperature and humidity conditions, it was shown that ionic impurities were generated after water absorption had taken place at high temperature (100 °C). These ions, which can move under DC electric field (≈ 8kV/mm), were detected near the electrodes where they accumulated [17]. Actually, from PEA measurements coupled with external current measurements it was shown that the formation of a space charge is detectable after a polarization period of several hours (150 h, 15 kV/mm) but only below the glass transition temperature [18, 19]. Above this temperature, the effect due to the dipolar polarization was found to be important. The surface charges that remain on the electrodes after short-circuit are combinations of dipole and space charge induced charges. The rise in the external current also supports the fact the injected charges contribute more to an increased DC conduction than to forming a field reducing space charge region at the injection contact.

In the present work, two kinds of samples of epoxy resin made of an Araldite CY1301 and the hardener HY1300 have been prepared to work under divergent and uniform field configuration at room temperature, i.e. below the glass transition temperature. The paper is organized as follows. The experimental details of sample preparation and EL detection set-up are given in a first part. Divergent and uniform field experiments are reported and discussed in the second and third parts respectively.

2 EXPERIMENTAL

2.1 EPOXY RESIN

The epoxy resin used is a non-vinyl polymer made of a Bisphenol-A containing reactive solvent and hardener that provides molecules with reactive amine groups. The base resin is essentially a mixture of Diglycidyl ether of Bisphenol-A (DGEBA) and Iso-Octyl Glycidyl Ether (IOGE). The polymerization is made at room temperature, which is one of the advantages of this product that allows a simple molding process. After polymerization, the glass transition temperature of the samples was measured by Differential Scanning Calorimetry method and found to be 42+/-2 °C [20]. The polymerized epoxy resin is transparent and sheets of material remain semi-flexible.

2.2 SAMPLE FOR DIVERGENT FIELD EXPERIMENTS

The divergent field geometry was created by molding into the resin a network of gold-plated tungsten wires of 5 μm in radius. They are separated by a distance of about 1 mm and are considered parallel and positioned in the middle of the bulk of a 290 μm-thick sample of epoxy resin (see Figure 1). The number of straight wires was 15. A special mold was used to maintain the wires in their position during the molding procedure. The curing process was achieved in 48 h. Once the samples have been made, a microscopic observation of the set of wires was performed. The absence of voids in the bulk and close to the wires was checked, as was the parallelism between the wires. The voltage was applied between the wires and the surfaces of the sample on which a semi-transparent layer of gold 300 Å-thick and 35 mm in diameter was deposited by cold sputtering. The periphery of the metallised layer was covered with silicon rubber to prevent stray light from the uncontrolled geometry of the metal in this region. The EL was detected through the upper layer on top of which a ring electrode was placed.

2.3 SAMPLE FOR UNIFORM FIELD EXPERIMENTS

The mold, made of polished aluminum plates and plastic spacers, was filled with the viscous liquid from one side [20]. After mixture of the base resin and hardener, the hardening time of about 30 min allowed the preparation of films sample of thickness between 50 μm and 150 μm. Semi-transparent gold layers were deposited onto both surfaces of the film. As for the divergent field experiment, the EL was detected through one electrode, the high voltage being applied to a ring electrode in contact with the layer.

2.4 SET-UP FOR ELECTROLUMINESCENCE DETECTION

The samples were placed on a lower cylindrical electrode in contact with a thermalized sink in a chamber where a high vacuum ($<10^{-4}$ Pa) was produced to remove oxygen and humidity. Divergent field experiments were performed at atmospheric pressure by introduction of dry nitrogen. Uniform field experiments were performed under vacuum to prevent discharges in the ambient at the highest voltage level of 20 kV, as described elsewhere [21, 22]. The emitted light was measured using a

photomultiplier (PM) working in the photo-counting mode. Although the average PM noise remained stable during a set of experiments, it can vary between 5 and 10 counts per second depending on the time the PM spent in total darkness before the specific experiment. It is therefore necessary to measure it precisely before each experiment. The PM has a flat spectral response in the wavelength domain extending from 300 nm to 800 nm. An ammeter was used to simultaneously record the charging-discharging current when performing DC experiments.

3 RESULTS AND DISCUSSION

3.1 DIVERGENT FIELD

Estimation of the Laplacian field distribution in the wire system has been carried out in order to determine a reasonable range of variation of the high voltage pulse amplitude. This was achieved by using a simulation based on the method of finite element already presented for similar geometries [23]. The potential is applied to the wires whereas both surfaces are grounded. This field will be called $E_{electrostatic}$ and is reported in Figure 2. Using a voltage of 3 kV leads to field of 120 kV/mm at the wire surface. The maximum voltage applied to the wire system was consequently limited to 3 kV to prevent breakdown after a few trials.

3.1.1 SINGLE PULSE EXPERIMENT

The first experiment was performed in order to determine the EL dependence on voltage amplitude and polarity. To do so, a single rectangular pulse lasting for t_{pol}= 200 ms was applied (Figure 3a). The first set of measurements recorded the number of photons emitted when the voltage was increased from V_{pol}= 0 to +/-3 kV. The light is only detected as the pulse is switched on or off, as shown in Figure 4a. In other words, the light is detected only on a step voltage, and the amount of light is the same during the positive (dV/dt>0) or negative (dV/dt<0) fronts (Figure 4b). The light was observed whatever the polarity of the applied voltage above +/-0.5 kV corresponding to a field of +/-20 kV/mm. The light detected rises with the increase of the applied voltage in a linear way. However, the absence of continuous light emission during constant voltage is noticeable even above a field of 100 kV/mm. Similar results were obtained with both polarities of voltages (see Figure 5). In the following sections, absolute values of voltage and electric field will be reported since the result would be the same under either polarity.

Occurrence of EL on voltage fronts of an impulse seems to be typical as it has already been described in different materials, for example Polyethylene Terephthalate [24]. Such results can be interpreted as follows. Charges are injected through the interfacial barrier and gain a kinetic energy sufficient to impact some molecules. This process is likely to occur at the interface between the wire and the resin as the scattering length for injected carriers is likely to be higher than in the bulk resin. The injected charge has therefore a higher probability of acquiring a kinetic energy at the contact than in the bulk. Light emission can therefore occur when the excited molecules are reverting to their ground state. Application of the Field Limiting Space Charge model (FLSC) [25] has been envisaged [14] to describe the charge transfer. In such a model, a critical field above which charge carriers acquire a high mobility is defined. The high mobility state is maintained as long as the space charge cloud does not reduce the field close to the contact below the critical field. The results reported by using LIPP [14] tend to suggest that the injection of charge that reduces the fields below the critical value for high mobility occurs in less than 10 ms. This would be consistent with our results, which show no effect of the polarization time in the range t_{pol}= 200 ms to 60 s on the detected EL. Moreover, the order of magnitude of the critical field in epoxy has been reported in the range of 100 to 600 kV/mm [25]. This is clearly not consistent with the field above which EL is detected in our experiments (20 kV/mm). Our results are rather consistent with a model in which the carrier injection itself is controlled by the trapped space charge. Fast processes of detrapping can also be envisaged on the negative voltage front. In this case, the field created by the space charge drives the process of charge detrapping, with the effect of a rapid decrease of the field at the wire below the onset field for light emission. However, the absence of light means *neither* that no extra charges are injected during the polarization *nor* that all the charges have been extracted after the removal of the voltage. It means only that the critical conditions to excite EL are not fulfilled. It is the step voltage shape, i.e. dV/dt, that plays an important part, being directly associated with the injection current that excites the luminescence until this current is limited by the space charge build up.

3.1.2 MULTIPLE PULSE EXPERIMENT

A second set of experiments has been carried out to check for the existence of space charge accumulation during the application of the first pulse. The application of a sequence of small pulses of opposite polarity relative to the polarity of the main pulse (see Figure 3b) was intended to unravel the presence of the accumulated space charge through its effect on the local field. The pulse train could also act as a probe for the space charge. The amplitude V_{probe} of such pulses was fixed below +/-0.5 kV to ensure that the probes cannot create light emission on their own.

A typical EL obtained during pulse train application is shown in Figure 6. It appears clear that the EL decreases until it disappears at about 30 s. Since the field created by the space charge is added to the field associated with the pulse voltage, it aids detrapping and charge extraction. It has been observed

that even when no light is detected on the polarization pulse (V_{pol} < 0.5 kV) some light could be recorded on the pulse train. This means that charges have been injected without exciting luminescence. The decrease of luminescence observed over the sequence of pulses may be due to the extraction of charges by the pulses. However it could be due to a "natural" extraction of the charges that would have occurred without the pulses or it could be due to the slow spreading out of the space charge region by charge diffusion. All these processes will reduce the contribution of the space charge field to the total local field, and hence will reduce the level of luminescence.

To investigate the impact of the pulse train on the trapped space charge, the EL measured during the first pulse of the pulse train has been recorded as the time t_{lag} was increased (Figure 7). It can be seen that the observed trend is comparable to that shown in Figure 6. This means that the EL, and hence the space charge field, reduces over a similar period of time independently of the application of a probe pulse. It therefore appears that the probe pulses extract only a small fraction of the total trapped charge at the instant of the pulse. The decrease in EL must therefore be due either to the spreading out of the space charge region by diffusion or a slow non-luminescent extraction in the space charge field alone. Each pulse of the train therefore acts as a true probe of the space charge field at the instant of its application. In particular, EL is observed when the combined field of pulse and space charge exceeds some onset value. This tends to imply that EL requires the acceleration of charges to some specific kinetic energy.

The reproducibility of the experiment has been checked by performing four trials consecutively on the same sample. The data are shown in Figure 8a. Although the number of trials is limited and the dispersion rather strong, we have defined the time t_{end} at which there is no more EL detected on the pulse. It is derived from Figure 8a as the average of the values obtained in each experiment. It can be seen in Figure 8b that this quantity has no dependence on the polarization time, meaning that the amount of accumulated charge does not change for polarization times between 200 ms and 60 s. This result is consistent with our previous finding derived from the single pulse experiment, meaning that the space charge is formed quickly and is limited by the injection.

3.1.3 SPACE CHARGE MODIFIED FIELD DISTRIBUTION

In order to check the consistency of the interpretation of EL excitation, we have carried out field computation taking into account a distribution of space charge around the wires. The latter are considered as cylinders of infinite length.

The field distribution due to the presence of the space charge alone (noted E_{SC}) has been computed by defining all the wires and surfaces to be at zero volts. The space charge volume is assumed to form a cylinder enclosing the wire. To take into account the diffusion of the charges into the bulk, the charge profile has been chosen to have a Gaussian shape with a characteristic radial width r and a maximum

charge density ρ_0. The equation giving the charge density as a function of the radial distance from the wire axis can be written as:

$$\rho(x) = \rho_0 \exp\left[-\left(\frac{x - x_{wire}}{r}\right)^2\right] \qquad (1)$$

where r is the characteristic penetration depth of the charge and ρ_o the maximum charge density.

The characteristic radial penetration of the charges has been estimated from space charge detection in the LIPP experiment, which gives a value of about 10 μm. In our sample, space charge has been detected by using PEA [26]. It was observed that they remain close to the surface of the wires within the limit of the spatial resolution. Hence, the value r = 20 μm corresponding to the characteristic penetration of charges from the wire axis has been used.

Using these approximations, it is possible to estimate the value of the field while the voltage is applied to the wires in presence of a space charge. This field corresponds to the addition of the electrostatic field to the field due to space charge, i.e.:

$$E = E_{electrostatic} + E_{SC} \qquad (2)$$

The value of the onset field for EL has been determined by calculating the field at which EL is first detected and is 20 kV/mm in our experiments. The space charge density needed to reduce the field at the wire surface below the onset field for EL excitation has been computed for different values of the applied voltage. As shown in Table 1, these values spread from 20 to 100 $C.m^{-3}$ depending on the voltage level. According to the proposed interpretation of luminescence excitation, the space charge will be formed around the wire within a few milliseconds, leading to a field reduction at the wire surface. The relevant situation is described in Figure 9 for an applied voltage of 2.5 kV. The electrostatic field is given as well as the space charge mediated field when the charge density is just enough to reduce the field at the wire surface to the level of the EL excitation field. The occurrence of electroluminescence during the negative voltage step of the square pulse has been ascribed to the extraction of trapped carriers towards the wire under the effect of the space charge field. The field magnitude generated by the space charge at the surface of the wire supports this interpretation as shown in Table 1. It can be seen that in every case, the space charge is able to generate a field that is higher than the field needed to excite the luminescence. This confirms our interpretation of the process of luminescence excitation.

The charge density derived from this study is clearly higher, but in the same range as the one measured in LIPP experiments performed on similar samples [14]. This is not surprising at all since LIPP measurements were performed 20 ms after the end of the pulse. They give therefore information

on the residual charges trapped in the material whereas EL experiments are sensitive to the charges that are extracted during the application of the negative voltage step of the square pulse. Analysis of the decay of the LIPP signal allows the derivation of the order of magnitude of the depth of the trapping levels that control the charge dissipation process 20 ms and more after the application of the pulse. It was found to be of the order of 1eV [16]. Charges extracted during the application of the negative step are located in shallower trapping centers (<1 eV). It was also shown that the decay of the observed space charge subsequent to short-circuit of the surface electrodes to the wires was consistent with detrapping and extraction of charges at the wires. It therefore seems most likely that the decay of the EL signal during the probe pulse experiments is primarily due to non-luminescent charge extraction occurring when the local space charge field is below the EL onset level.

3.2 UNIFORM FIELD

A DC field was used in order to look for a possible correlation between the excitation of electroluminescence, the conduction process and space charge distribution throughout the sample.

3.2.1 ELECTROLUMINESCENCE DETECTION

A step ramp technique was used to detect the EL on 55 μm-thick samples. The dwell time was 300 s on the ascending ramp and 150 s on the descending ramp. The field step was 9 kV/mm. The EL was averaged over time after the first 50 s at each step. In the experiment, the sample was cycled to progressively higher applied fields. As shown in Figure 10, continuous EL was observed to occur above 175 kV/mm when ramping up. When the voltage was ramped down, EL ceased at a higher field, of the order of 250 kV/mm.

The existence of a continuous EL under DC field can be explained either by the existence of hot carriers that can be accelerated to high kinetic energies, or by bipolar injection from anode and cathode, charge migration and the formation of recombination domains. Analysis of conduction processes and investigation of the field dependence of space charge profiles provide a way to tackle the problem. Combined EL and current measurements performed on different polymeric materials have shown a good correlation between the onset for permanent EL excitation and a change in the conduction mechanism as denoted by a steep increase of the slope of the current-field characteristic in a log-log representation [27]. Similarly, investigation of the spatial distribution of the space charge at different fields revealed that the continuous EL is seen after bipolar injection from cathode and anode, thereby pointing towards a mechanism of excitation due to charge recombination [28, 29]. We have developed a similar approach here by investigating the external current and space charge profile (using the pulsed electro-acoustic technique) at different fields up to the range of field where electroluminescence was detected.

3.2.2 CURRENT MEASUREMENTS AND ANALYSIS

Current measurements were performed in vacuum on a gold-metallised 55 μm-thick sample by using a polarisation/depolarisation procedure. The voltage was applied for one hour, the sample being short-circuited at the end of the polarization time for the same time before repeating the experiment under a higher voltage (step increase of the field was 18 kV/mm). Charging and discharging currents vs. poling field are shown in Figure 11(a) and 11(b) respectively. Considering figure 11(a), the charging current decreases continuously in time up to about 100 kV/mm indicating that the recorded values are dominated by the transient component, the DC conduction process not being reached by the end of the poling period. Above this field, there is a clear contribution from the conduction current and the current level taken at 3600 s can be considered as an approximation to the conduction component. The current values obtained at the end of the polarization time are plotted versus field in Figure 12. It shows a change from a transient dominated current with a linear increase in field (< 100 kV/mm) to a conduction-dominated current with a supralinear increase in field (> 100 kV/mm). Considering figure 11(b), the discharging current never decays exponentially as would be the case for a pure Debye behavior of the relaxing dipoles. A dipolar relaxation time τ can be derived from the discharging current plot by using the change in slope in a log-log representation. The time dependence of the current is t^{-n} for $t < \tau$ and $t^{-(m+1)}$ for $t > \tau$ [30]. Taking the curve obtained at the lowest field (18 kV/mm) to ensure that the data are relevant to a linear regime, one finds τ=278 s which is equivalent to a response frequency of 5.7×10^{-4} Hz. The value of the power exponent n was found to be 0.69 from the current which agrees very well with the estimate of n=0.73 derived from the frequency dependence of a relaxation process observed in the dielectric response [20] the peak for which must lie below our lowest frequency of observation $f = 10^{-3}$ Hz. A similar value (n = 0.78) is obtained from the polarization current. It is therefore clear that the transient current can be identified with a relaxation process observed by dielectric spectroscopy.

The charging-discharging current analysis emphasizes the importance of slow transients due to dipole orientation that dominate the charging currents below 100 kV/mm, and probably also contribute to it in the transition zone defined in Figure 12. When comparing the onset field for EL to the shape of the characteristic shown in Figure 12, it is clear that EL is detected at a field corresponding to the non-linear regime of the current, but it is not possible to associate the EL onset to a specific change in the characteristic. This could be because the transient smeared out the expected transition in the conduction mechanism. Alternative explanations could be that the EL detection is sensitivity-limited, or that there is not such a change in the conduction process. Further longer-term recording of current and electroluminescence is needed to bring a definite answer to this question.

3.2.3 SPACE CHARGE DISTRIBUTION ANALYSIS

Space charge measurements were performed by the pulsed electro-acoustic technique [32] at various DC-voltages varying from ~10 to 180 kV/mm. Measurements were performed in air at room temperature. The sensitivity limit of the system is about 0.1 $C.m^{-3}$ and its spatial resolution of the order of 10 μm. The electrodes in contact with the films were semiconducting carbon-filled polyethylene wrapped in aluminum foil (high voltage electrode, anode) and aluminum (cathode) electrodes of the PEA system. We have followed the same experimental protocol as during the current measurements taking space charge profiles at different times during polarization (1 hour of duration, PEA profiles taken in volt-on) and depolarization (1 hour of duration), at different field levels. A 110 μm-thick sample and a 1 kV voltage increment (9 kV/mm in field) were used.

Both space charge and dipolar orientation are expected to contribute to the PEA response. Dielectric spectroscopy [31] has revealed the contribution of three polarization processes, one of which has been identified in the time dependence of the current. The contribution of dipolar orientation to the PEA response corresponds to a pure capacitive signal (only surface charge) as far as the dipolar orientation can be considered as uniform throughout the depth of the sample. Figure 13 shows the charge profiles obtained at the end of the polarization stage during volt-on and at different times during volt-off, for a field of 18 kV/mm. The profile taken 15 s after volt-off clearly shows the existence of homocharge regions of equivalent amplitude and penetration depth. This is shown by the image charges on the electrodes that have opposite signs to the space charge. Subsequent charge profiles show a decrease in the amplitude of the peaks associated with the image charges together with a concomitant shift in the position of the "internal" charge peaks; this unambiguously shows a fast relaxation of the space charge. The profile taken 30 min after volt-off has the same shape as the profile observed in volt-on. This shows that the injected homo-charges have relaxed within 30 min, the charge profile at this time corresponding to a pure dipolar response.

Similar PEA profiles are shown in Figure 14 for fields of 72 kV/mm, 100 kV/mm and 130 kV/mm.

The following remarks can be made:

-Space charge dissipation is seen in every case through the decrease in amplitude of the image charge peaks. However, there may be still space charge in the material even in the absence of image charge peaks if the latter is cancelled by the contribution of the dipolar response [33]. A space charge-free situation would correspond to a pure capacitive response, i.e. the position of the maximum of the charge peak must be in correspondence with the capacitive signal observed under volt-on. That is clearly not the case 30 min after volt-off. The space charge relaxation time is much longer than that derived from the decay of the image charge peak. This is confirmed by the charge profile recorded at 720 min at 100 kV/mm (see Figure 14b). On the cathode side, it can be seen that the signal

corresponds to a pure capacitive response meaning that the negative space charge has been dissipated here. The same does not hold on the anode side for reasons discussed below.

-The positive and negative charges do not dissipate with the same kinetics. This can already be seen in Figure 13 where the profile taken at 30 s shows no image charge on the cathode side whereas an image charge can still be seen on the anode side. This observation is confirmed by the profiles at higher fields. Consideration of the profile taken 15 s after volt-off (130 kV/mm) shows that positive (at the cathode) and negative (at the anode) image charge peaks are of equal amplitude suggesting equivalent amounts of injected positive and negative charges. Profiles taken at 30 s show a strong asymmetry between the image charge peaks denoting a faster removal of negative charges as compared to positive ones. This could be due to a difference in behavior of positive and negative charges at the epoxy/electrode contact.

-Positive charges are seen to penetrate into the specimen bulk. Penetration of positive charges is seen at 100 kV/mm and confirmed at 130 kV/mm.

As expected, the charge distribution in the epoxy is the combination of dipolar and space charge contributions. It is found that space charge dissipation is faster than dipolar relaxation which appears in conflict with the dielectric response that shows that any polarization should have relaxed within a few minutes (the low frequency peak corresponds to a relaxation, time of ~300 s). The two results can be reconciled once one realizes that the internal space charge is able to polarize the material, and hence that the space charge and dipolar contributions would not be independent. This would also provide an interpretation for the fact that space charge can be present in the bulk and its image charge not detected at the electrodes due to its cancellation by the dipolar induced charge [33]. One important finding regarding electroluminescence excitation is that space charge has been shown to be injected in to the sample at 18 kV/mm. Earlier results also show that space charge could be injected after one hour of voltage application at fields as low as 10 kV/mm [20]. These results lend support to the contention that the minimum field of 20 kV/mm for the detection of transient EL in the divergent field experiments is not the onset field for charge injection, but instead the onset field for the electroluminescence mechanism itself. That is, charges are injected at fields below 20 kV/mm but only acquire sufficient kinetic energy to excite EL at fields greater than or equal to 20 kV/mm.

As the applied field is increased the amount of charge injected increases. The most important point to note, however, is the tendency for positive charge to penetrate into the bulk of the sample, which starts to appear at 100 kV/mm and above. The positive charge density in the bulk is still small (< 1 C.m^{-3}) and does not extend to the negative homocharge at the cathode. If, however, such a penetration were to become more pronounced and more extensive at higher fields it could provide a means for continuous EL via charge recombination as in XLPE [29]. This has not been definitively determined here because

experiments at the onset field for continuous EL (175 kV/mm) could not be carried out for this sample that broke down before this field level.

To confirm this contention we have carried out an experiment at 20 kV (E = 180 kV/mm) on a different sample using a different protocol. The voltage was raised to E = 180 kV/mm by steps of 9 kV/mm lasting 5 min. The sample therefore has a different electrical history to the previous one. The PEA results given in Figure 15 show that at this field which is equal to the onset field for continuous EL, positive space charge has penetrated the bulk to the negative homo-charge region, thereby facilitating charge recombination as in XLPE [29].

4 CONCLUSION

Electroluminescence excitation mechanisms in epoxy have been discussed in divergent and uniform fields. The divergent situation was produced around a set of molded wires by applying square voltage pulses not less than 100 ms in duration. The electroluminescence was evidenced during the fronts of the applied voltage being of equal intensity upon application or removal of the voltage. The EL was not detected during the plateau of the pulse, and it was of equal intensity for different polarities of the applied voltage. The interpretation of the EL excitation involves fast charge injection (dynamic << minimum pulse duration) and charge trapping leading to a field-reduction at the wire surface below the minimum field needed to excite the electroluminescence. Charge accumulation was found in multiple pulse experiments where small voltage pulses, of a polarity opposed to the polarity of the main pulse, and of amplitude less than the one needed to excite the EL, were used as a probe. It was shown that the EL ceased to be excited by the probe pulses when they are applied after a certain time, of the order of 60 s, showing that space charge had dissipated in the region around the wire. The proposed interpretation for EL excitation is supported by field computation in the presence of space charge. PEA analysis of charge injection in uniform fields showed that homo-charge injection occurred at fields below the onset field for the transient EL, and hence confirmed that this field is associated with the EL mechanism itself.

A uniform field situation was produced using films of epoxy submitted to DC fields. Electroluminescence, charging/discharging current and space charge profiles using the pulsed electro-acoustic technique were recorded at different field levels. It was shown that a continuous EL level is detected at 175 kV/mm. This is clearly associated with a non-linear conduction regime but the contribution to the external current of the dipolar orientation prevents the analysis of the conduction mechanism based on short-term current recording. Further work will be carried out to elucidate the correlation between conduction and EL onset. PEA analysis showed that positive and negative homo-charge built-up is effective at field of 20 kV/mm. Penetration of positive charges into the bulk is

evidenced upon field increase pointing towards bi-polar charge recombination as the driving mechanism for continuous EL excitation in epoxy.

The large difference in EL excitation under impulse (20 kV/mm) and DC (175 kV/mm) fields is due to the difference in excitation mechanisms. Injection and acceleration of carriers at the metal/dielectric interface have been proposed in the former case whereas bi-polar charge injection, transport and recombination are thought to be the driving mechanisms under DC. Moreover, the two EL are of a different nature being a fast transient occurring at voltage fronts in the divergent situation, and a continuous process occurring under constant applied field in the uniform one.

The difference of field configurations (divergent vs. uniform) does not appear influential as for the onset for charge injection. Homo-charge accumulation has been found at ~20 kV/mm in both kinds of experiment. Similarly, the order of magnitude of the homo-charge detected after volt-off in uniform field experiments (5 to 20 $C.m^{-3}$) is consistent with the charge needed to generate the EL (10 to 100 $C.m^{-3}$) under pulse voltage excitation in divergent field conditions.

ACKNOWLEDGEMENT

The authors thank the Royal Society and the CNRS for the provision of a Joint Research Scheme grant which facilitated the collaboration. JCF would like to thank the University of Leicester for the provision of study leave.

REFERENCES

[1] "Electroluminescence", Topics in Applied Physics, Edited by J.I. Pankove, Springer-Verlag, New York, 1977.

[2] "Organic Electroluminescent Materials and Devices", Edited by S. Miyata and H.S. Nalwa, Gordon and Breach Publishers, 1997.

[3] C. Laurent, "Optical Pre-Breakdown Warnings in Insulating Polymers", International Conference on Conduction and Breakdown in Solid Dielectrics, Västeras, Sweden, pp. 1-12, 1998.

[4] "Electrical Degradation and Breakdown in Polymers", L.A. Dissado and J.C. Fothergill, Edited by G.C. Stevens, Peter Peregrinus Ltd, 1992.

[5] H. R. Zeller, "Non Insulating Properties of Insulating Materials", Conference on Electrical Insulation and Dielectric Phenomena, Knoxville, USA, pp. 19-47, 1991.

[6] C. Laurent, F. Massines and C. Mayoux, "Optical Emission due to Space Charge Effects in Electrically Stressed Polymers", IEEE Trans. Diel. EI, Vol. 4, pp. 585-603, 1997.

[7] Y. Shibuya, G. Colleti, S. Zoledziowski and J. H. Calderwood, "Prebreakdown Light Emission in Epoxy Resin", International Symposium on HV Engineering, Zurich, Switzerland, pp. 612-616, 1975.

[8] K. Nakanishi, S. Hirayabashi and Y. Inuishi, "Phenomena and Mechanisms of Tree Inception in Epoxy Resins", IEEE Trans. EI, Vol. 14, pp. 306-314, 1979.

[9] T. Bauman, B. Fruth and F. Stucki, "Charge Injection and Electroluminescence in the Prestate of Dielectric Ageing", Fifth Intern. Symp. on High Voltage Engineering, Braunschweig, Germany, pp. 1-4, 1987.

[10] G.C. Stone and R.G. VanHeeswijk, "The effect of Polarity and Surge Repetition Rate on Electroluminescence in Epoxy", Conference on Electrical Insulation and Dielectric Phenomena, Leesburg, USA, pp. 173-179, 1989.

[11] J.V. Champion, S.J. Dodd and G.C. Stevens, "Long-term Light Emission Measurement and Imaging During the Early Stages of Electrical Breakdown in Epoxy Resin", J. Phys. D: Appl. Phys., Vol. 27, pp. 604-610, 1994.

[12] J.V. Champion, S.J. Dodd and G.C. Stevens, "Quantitative Measurement of Light Emission During the Early Stages of Electrical Breakdown in Epoxy and Unsaturated Polyester Resins", J. Phys. D: Appl. Phys., Vol. 26, pp. 819-829, 1994.

[13] R. Coisson, C. Paracchini and G. Schianchi, "Electroluminescence in an Epoxy Resin", J. Electrochem. Soc., Vol. 125, pp. 581-583, 1978.

[14] O. Naz-Paris, "Etude d'Isolants soumis à des Champs Divergents par une Mesure Directe des Distributions de Charges Injectées", Thèse de doctorat, Université Paris VI, 2000.

[15] O. Naz, J. Lewiner, T. Ditchi and C. Alquié, "Study of Charge Injection in Insulators Submitted to Divergent Fields", IEEE Trans. Diel. EI, Vol. 5, pp. 2-8, 1998.

[16] L.A. Dissado, O. Paris, T. Ditchi, C. Alquié and J. Lewiner, "Space Charge Injection and Extraction in High Divergent Fields", Conference on Electrical Insulation and Dielectric Phenomena, Austin, USA, pp. 1, pp. 23-26, 1999.

[17] T. Iizuka, Y. Takai, K. Fukunaga, T. Maeno, "Measurements of Space Charge Distribution in Epoxy Resin After Water Absorption Treatment", Conference on Electrical Insulation and Dielectric Phenomena, Mineapolis, USA, pp. 41-44, 1997.

[18] K. Fukunaga and V. Griseri, "Space Charge and External Current Measurements of a Filler-Free Epoxy", Trans. IEE Japan, Vol. 120-A, pp. 667-668, 2000.

[19] K. Fukunaga, T. Maeno and V. Griseri, "Space Charge Observation of a Filler-Free Epoxy Resin", Conference on Electrical Insulation and Dielectric Phenomena, Victoria, Canada, pp. 125-127, 2000.

[20] V. Griseri, "The Effects of High Electric Fields on an Epoxy Resin", Degree of Doctor of Philosophy, University of Leicester, October 2000.

[21] G. Teyssedre, D. Mary, C. Laurent and C. Mayoux, "Optical Emission due to Space Charge Recombination in Insulating Polymers: an Insight into Electrical Ageing", Space Charge in Solid Dielectrics, Dielectric Society Ed, UK, pp. 285-302, 1998.

[22] D. Mary, M. Albertini and C. Laurent, "Understanding Optical Emissions from Electrically Stressed Insulating Polymers: Electroluminescence in Poly(Ethylene Terephthalate) and Poly(Ethylene 2, 6-Naphthalate) Films", J. Phys. D: Appl. Phys., Vol. 30, pp. 171-184, 1997.

[23] O. Paris, J. Lewiner, T. Ditchi, S. Holé and C. Alquié, "A finite Element Method for the Determination of Space Charge Distributions in Complex Geometry", IEEE Trans. Diel. EI., Vol. 7, pp. 556-560, 2000.

[24] K. Kojima, Y. Takai and M. Ieda, "Electroluminescence in Polyethylene Terephthalate (PET) I. Impulse Voltage", Jpn. J. Appl. Phys., Vol. 21, pp. 860-864, 1982.

[25] T. Hibma and H. R. Zeller, "Direct Measurement of Space-Charge Injection from a Needle Electrode into Dielectrics", J. Appl. Phys., Vol. 59, pp. 1614-1620, 1986.

[26] K. Fukunaga, unpublished results.

[27] G. Teyssedre, D. Mary, G. Tardieu and C. Laurent, "AC and DC Electroluminescence in Insulating Polymers and Implication for Electrical Ageing", submitted to J. Appl. Phys.

[28] J. L. Augé, G. Teyssedre, C. Laurent, T. Ditchi and S. Holé, "Combined Electroluminescence and Charge Profile Measurements in Poly(ethylene-2, 6-naphthalate) under a DC Field", J.Phys.D: Appl.Phys., Vol. 33, pp. 3129-3138, 2000.

[29] G. Teyssedre, C. Laurent, G. C. Montanari, F. Palmieri, A. See, J. C. Fothergill and L. Dissado, "Charge Distribution and Electroluminescence in XLPE under DC field", submitted to J. Phys. D: Appl. Phys.

[30] A. K. Jonscher, "Universal Relaxation Law", Chelsea Dielectrics Press, London, 1996.

[31] V. Griseri, K. Fukunaga, C. Laurent, D. Mary, L. A. Dissado and J. Fothergill, "Charge injection, electroluminescence, and ageing of an epoxy resin in high divergent fields", Eighth International Conference on Dielectric Materials, Measurements and Applications, Edinburgh, UK, pp. 88-93, 2000.

[32] J. C. Fothergill, L. A. Dissado, J. Alison and A. See, "Advanced pulsed electro-acoustic system for space charge measurement", Eighth International Conference on Dielectric Materials, Measurements and Applications, Edinburgh, UK, pp. 352-356, 2000.

[33] V. Griseri, L. A. Dissado and K. Fukunaga, "The Effect of Space Charge Induced Dielectric Polarization upon Decay of a PEA Signal following Voltage Removal", Annual Meeting of the Dielectrics Society, Toulouse, France, 2001.

FIGURE CAPTIONS

Table 1 : Space charge modified field

ρ_0 is the charge density needed to reduce the field at the wire surface below the onset field for EL (20 kV/mm). E_{ES} and E_{sc} are the electrostatic field and the field induced at the wire surface by a charge of density ρ_0 respectively.

Figure 1 : Schematic of sample used for divergent field experiment

Figure 2 : Electrostatic field distribution around a wire

Wire at potential V. Sample surfaces at ground potential.

Arrows indicate increasing voltage : 250, 500, 1000, 2000, 2500, 3000 V

Figure 3 : Shape of voltage pulse in divergent field experiments

(a) Single pulse experiment, (b) Multiple pulse experiment

Variable parameters : V_{pol}, t_{pol}, t_{lag}

Fixed parameters : $|V_{probe}| = 0.5$kV, $\Delta t_{probe} = 0.1$ s, pulse probe frequency = 0.5 Hz

Figure 4 : Time and voltage dependence of EL in a single pulse experiment

(a) EL during a single pulse experiment : each data point represents the number of PM pulses counted during 10ms. Pulse due to the noise of the PM correspond to a level of 5 cps (counts per second). The signal exceeding this level is due to EL. It is clearly seen during the positive and negative fronts, whereas no EL is detectable under constant voltage. (b) EL counts during the step-up (triangle) and step-down (crosses) fronts of the applied voltage.

Figure 5 : EL versus voltage polarity.

EL count on positive (step-up) and negative (step-down) voltage fronts have been added. Squares : positive polarity; circles : negative polarity.

Figure 6 : Typical EL response obtained on a pulse train as a function of time after main pulse step-down. (t_{lag} = 1 s, V_{pol} = 2.75 kV, t_{pol} 45 s).

Figure 7 : EL measured during the first pulse of the train versus t_{lag}

(V_{pol} = 2.5 kV, t_{pol} = 5 s)

Figure 8 : Results of several trials performed on the same sample

(a) EL on pulse train versus time after main pulse step-down (t_{pol} = 45 s, V_{pol} = 2.75kV, t_{lag} = 1 s). t_{end} is the time of luminescence vanishing. (b) Statistical dispersion on t_{end} versus polarization duration.

Figure 9 : Space charge field for different space charge density.
Solid line : $\rho = 0$, dashed lined : $\rho = 50$ C.m^{-3}, doted line : $\rho = 75$ C.m^{-3}

Figure 10 : Electroluminescence as a function of field during
(a) ramp-up and (b) ramp down.

Figure 11 : (a) Charging and (b) discharging currents for different fields
Arrow indicates the increase of field : 18, 36, 72, 108, 144, 162, 180, 200 kV/mm

Figure 12 : Current-field characteristic obtained by plotting the charging current at 3600 s vs field

Figure 13: Space charge profile at 18 kV/mm. The volt-on profile was obtained at the end of the polarization period. The volt-off profiles were obtained at different times as indicated.

Figure 14: Space charge profiles for different fields : (a)-72 kV/mm, (b)-100 kV/mm and (c)-130 kV/mm. The solid line is the Volt-on signal (Y-scale x 0.2) measured at the end of the polarization period. The volt-off profiles were obtained at different times as indicated. Cathode on the left, anode on the right.

Figure 15: Space charge profile at 180 kV/mm. The field was increased in steps of 9 kV/mm lasting for 5 min. The volt-on profile was obtained at the end of the ramp-up. The volt-off profiles were obtained at different times as indicated. Cathode on the left, anode on the right.

Table 1 : Space charge modified field
ρ_0 is the charge density needed to reduce the field at the wire surface below the onset field for EL (20 kV/mm). E_{ES} and E_{sc} are the electrostatic field and the field induced at the wire surface by a charge of density ρ_0 respectively.

V_0 (V)	1000	1500	2000	2500	3000
E_{ES}(kV/mm)	40	60	80	90	120
E_{SC} (kV/mm)	-20	-40	-60	-70	-100
ρ_0 (C.m^{-3})	22	45	65	80	110

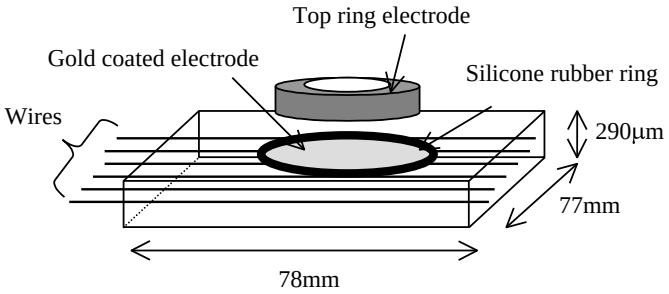

Figure 1 : Schematic of sample used for divergent field experiment

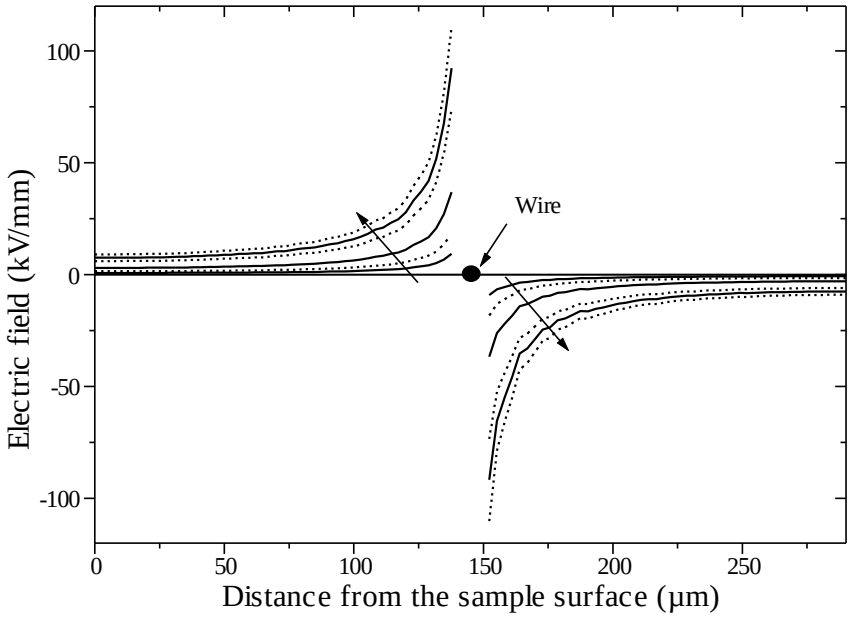

Figure 2 : Electrostatic field distribution around a wire
Wire at potential V. Sample surfaces at ground potential.
Arrows indicate increasing voltage : 250, 500, 1000, 2000, 2500, 3000 V

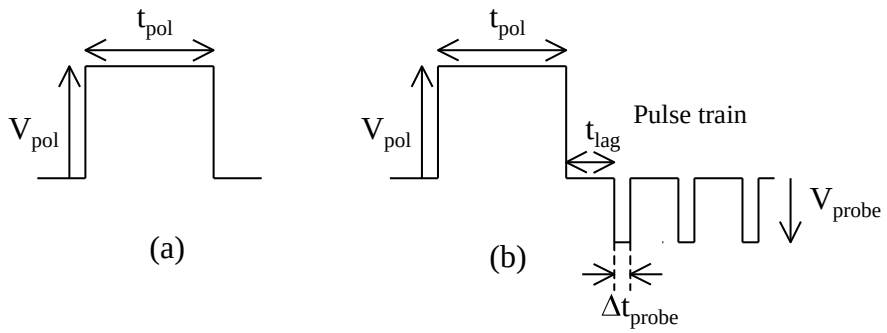

Figure 3 : Shape of voltage pulse in divergent field experiments
(a) Single pulse experiment, (b) Multiple pulse experiment
Variable parameters : V_{pol}, t_{pol}, t_{lag}
Fixed parameters : $|V_{probe}|$ = 0.5kV, Δt_{probe} = 0.1 s, pulse probe frequency = 0.5 Hz

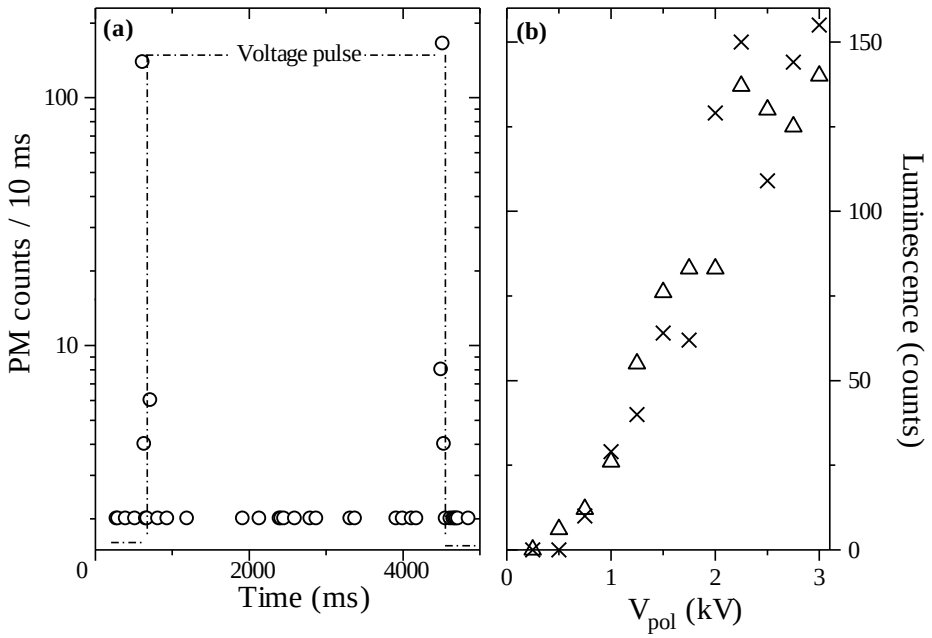

Figure 4 : (a) EL during a single pulse experiment : each data point represents the number of PM pulses counted during 10ms. Pulse due to the noise of the PM correspond to a level of 5 cps (counts per second). The signal exceeding this level is due to EL. It is clearly seen during the positive and negative fronts, whereas no EL is detectable under constant voltage. (b) EL counts during the step-up (triangle) and step-down (crosses) fronts of the applied voltage.

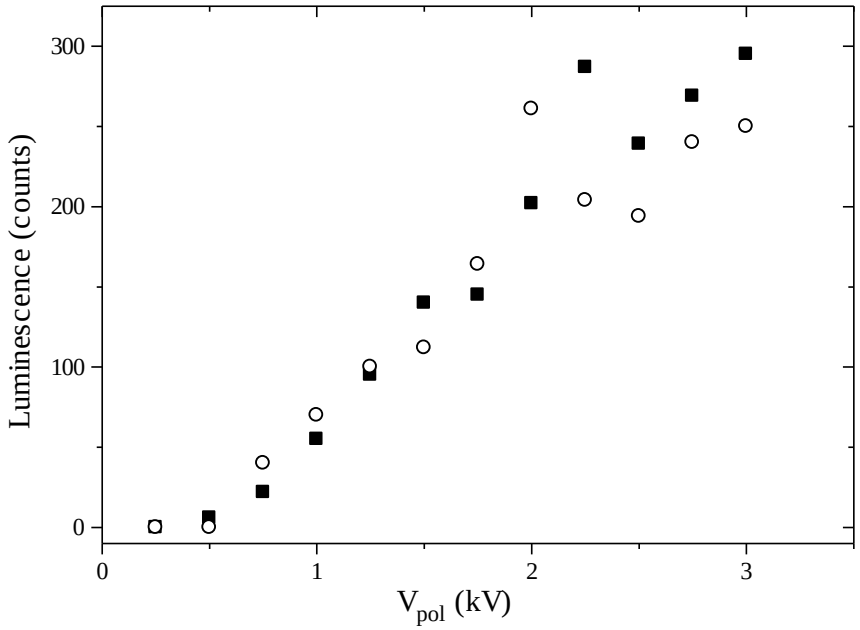

Figure 5 : EL versus voltage polarity EL count on positive (step-up) and negative (step-down) voltage fronts have been added. Squares : positive polarity; circles : negative polarity.

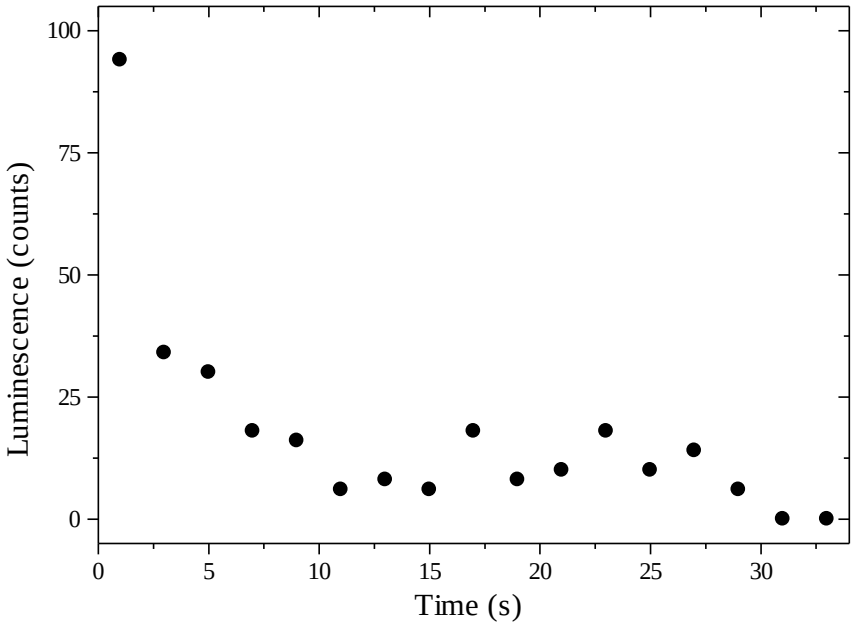

Figure 6 : Typical EL response obtained on a pulse train as a function of time after main pulse step-down (t_{lag} = 1 s, V_{pol} = 2.75 kV, t_{pol} 45 s)

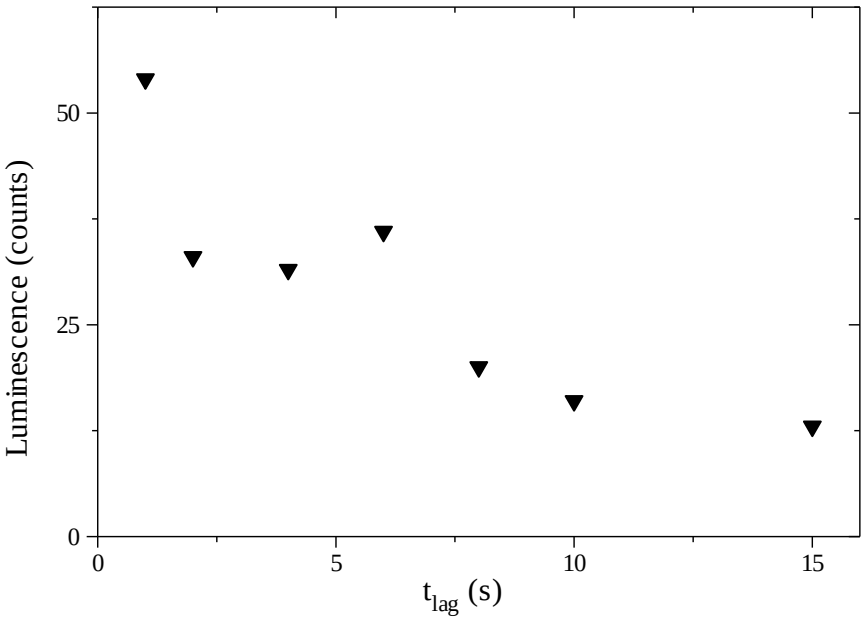

Figure 7 : EL measured during the first pulse of the train versus t_{lag}
(V_{pol} = 2.5 kV, t_{pol} = 5 s)

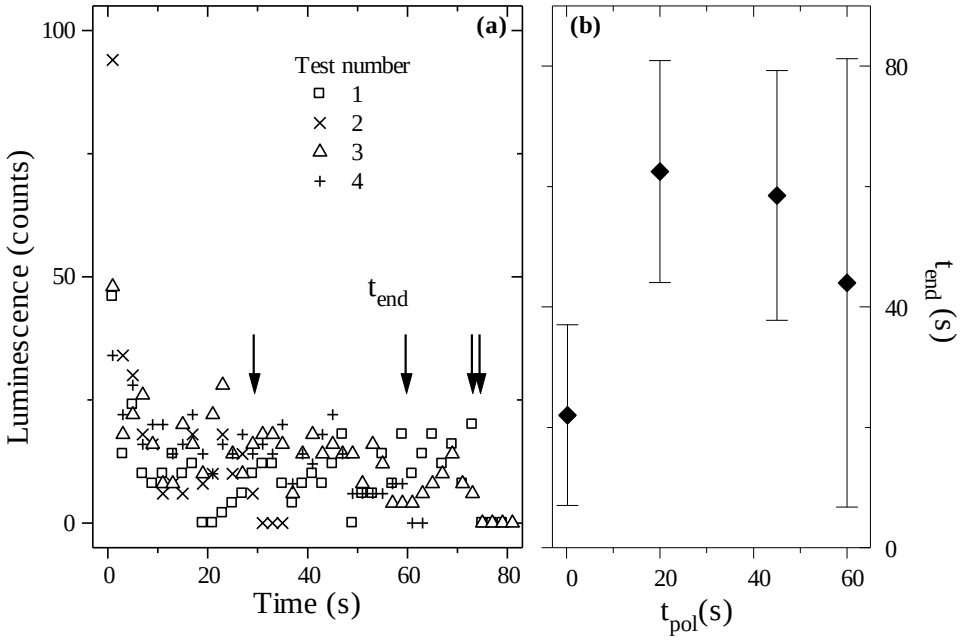

Figure 8 : Results of several trials performed on the same sample
(a) EL on pulse train versus time after main pulse step-down (t_{pol} = 45 s, V_{pol} = 2.75kV, t_{lag} = 1 s). t_{end} is the time of luminescence vanishing. (b) Statistical dispersion on t_{end} versus polarization duration.

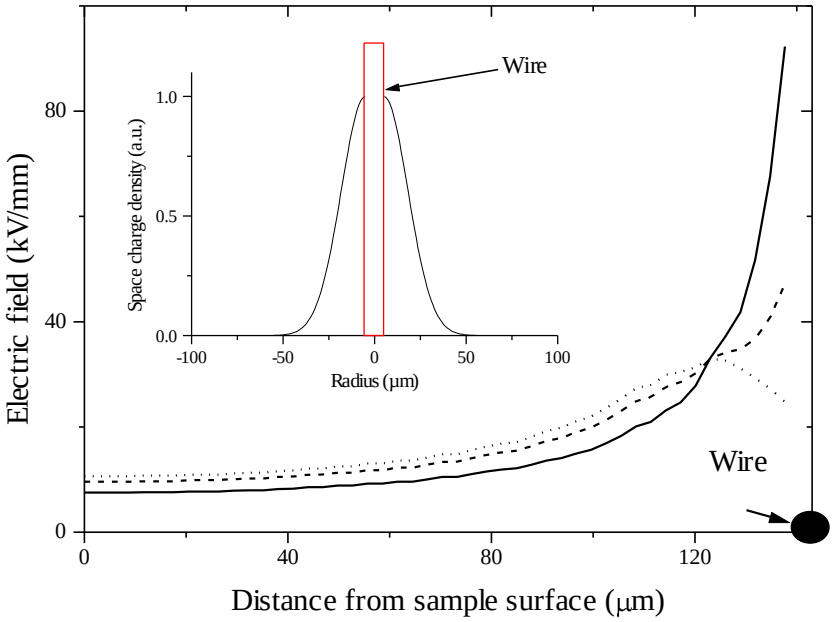

Figure 9 : Space charge field for different space charge density.
Solid line : $\rho = 0$, dashed lined : $\rho = 50$ C.m^{-3}, doted line : $\rho = 75$ C.m^{-3}

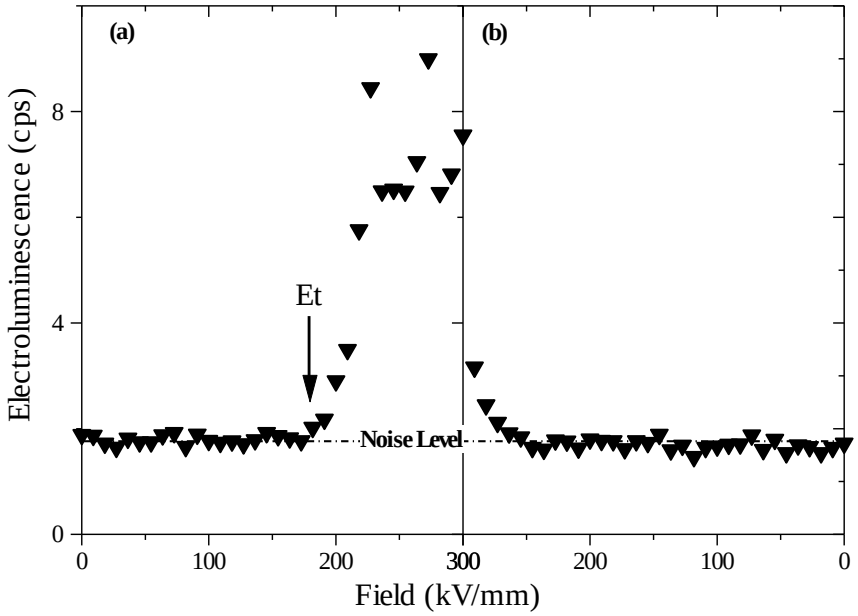

Figure 10 : Electroluminescence as a function of field during (a) ramp-up and (b) ramp down.

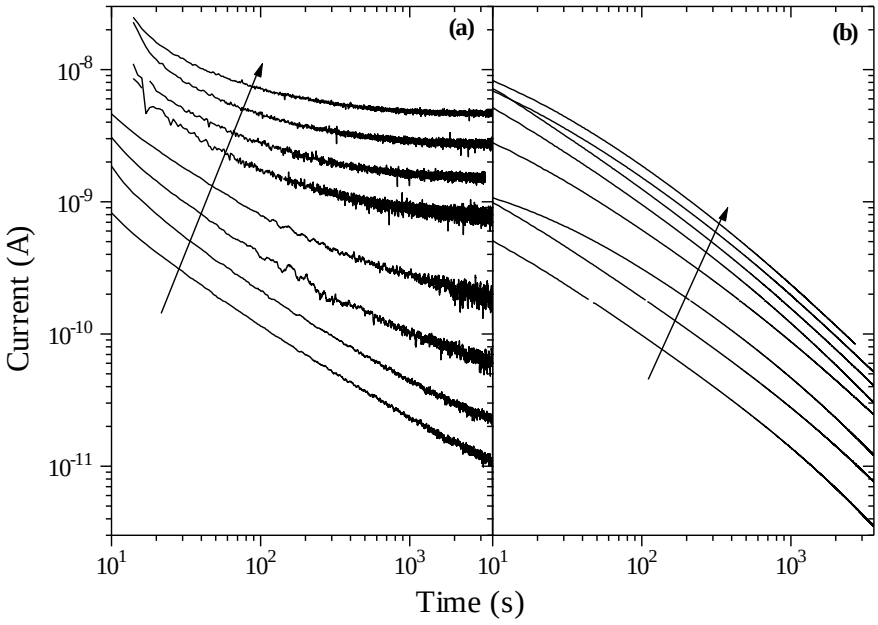

Figure 11 : (a) Charging and (b) discharging currents for different fields
Arrow indicates the increase of field : 18, 36, 72, 108, 144, 162, 180, 200 kV/mm

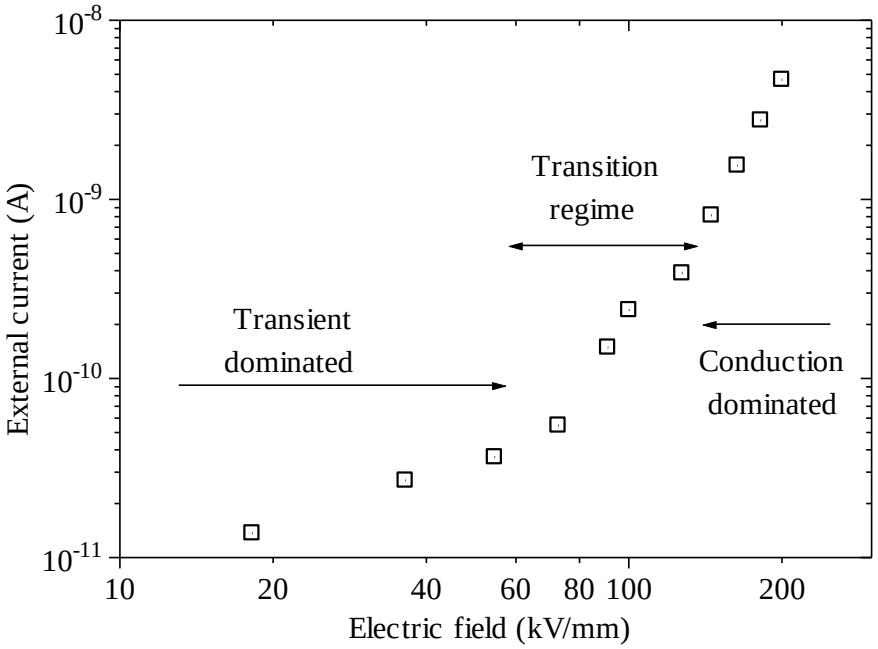

Figure 12 : Current-field characteristic obtained by plotting the charging current at 3600 s vs field

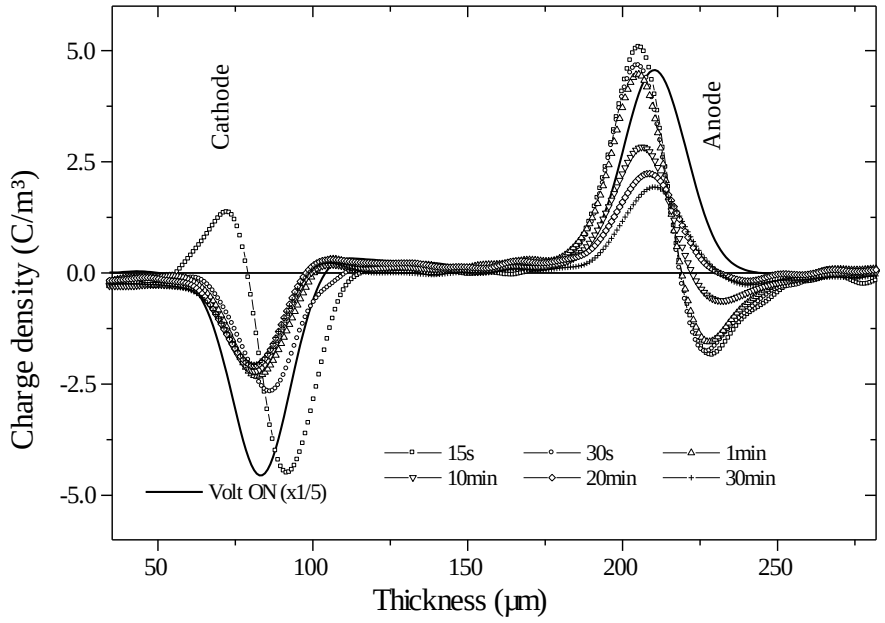

Figure 13: Space charge profile at 18 kV/mm. The volt-on profile was obtained at the end of the polarization period. The volt-off profiles were obtained at different times as indicated.

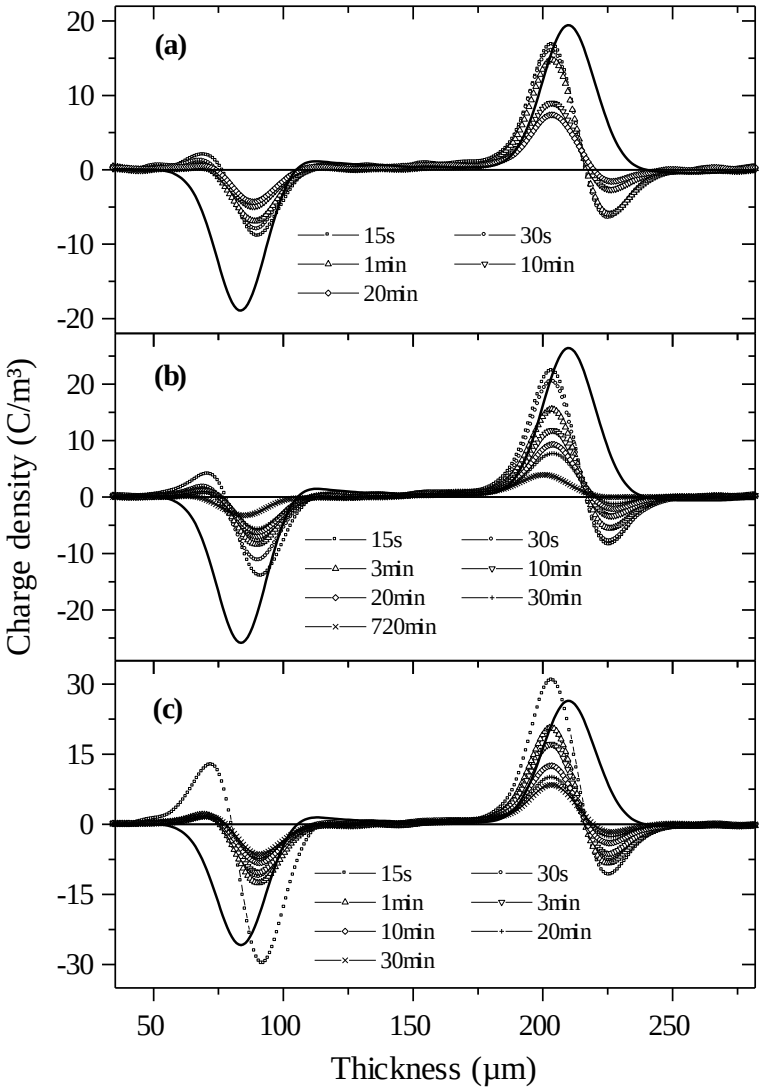

Figure 14: Space charge profiles for different fields : (a)-72 kV/mm, (b)-100 kV/mm and (c)-130 kV/mm. The solid line is the Volt-on signal (Y-scale x 0.2) measured at the end of the polarization period. The volt-off profiles were obtained at different times as indicated. Cathode on the left, anode on the right.

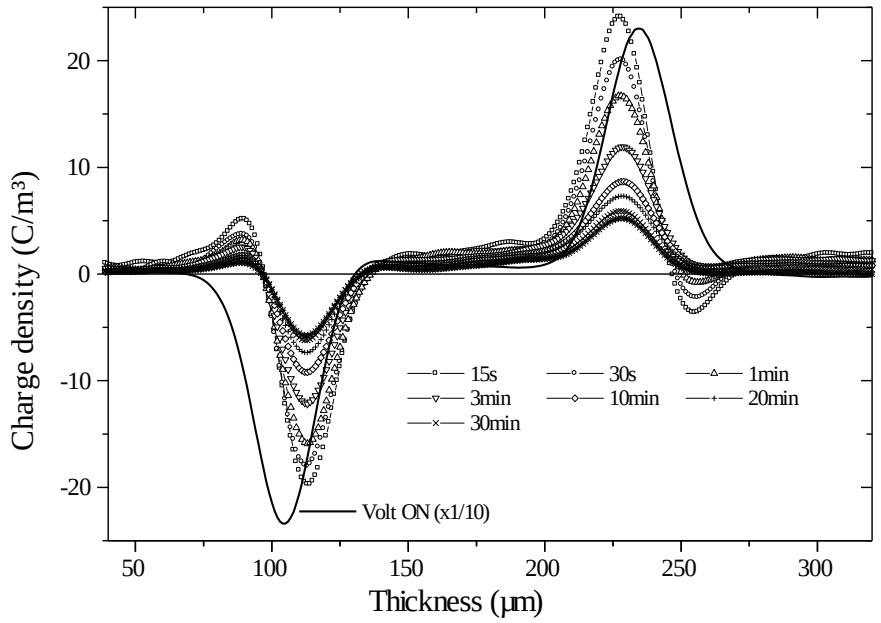

Figure 15: Space charge profile at 180 kV/mm. The field was increased in steps of 9 kV/mm lasting for 5 min. The volt-on profile was obtained at the end of the ramp-up. The volt-off profiles were obtained at different times as indicated.